Spring 1-1-2011

Modeling the Micro Behavior and Failure of Collagen Based Fibrous Materials

Spencer T. Hallowell
University of Colorado at Boulder, hallowell.spencer@gmail.com

MODELING THE MICRO BEHAVIOR AND FAILURE OF COLLAGEN BASED FIBROUS MATERIALS

by

SPENCER T. HALLOWELL
B.S. Bucknell University, 2010

A thesis submitted to the
Faculty of the Graduate School of the
University of Colorado in partial fulfillment
of the requirement for the degree of
Master of Science
Department of Civil and Architectural Engineering
2011

This thesis entitled:
Modeling the Micro Behavior and Failure of Collagen Based Fibrous Materials
written by Spencer T. Hallowell
has been approved for the Department of Civil and Architectural Engineering

Franck Vernerey
Committee Chair

Jon Dow
Committee Member

Date 12/2/2011

The final copy of this thesis has been examined by the signatories, and we
Find that both the content and the form meet acceptable presentation standards
Of scholarly work in the above mentioned discipline.

Hallowell, Spencer T. (M.S., Civil Engineering, Structures)

Modeling the Micro Behavior and Failure of Collagen Based Fibrous Materials

Thesis directed by Assistant Professor Franck Vernerey

The field of tissue engineering has expanded vastly over the last decade. Due to difficulties in testing tissues in vivo, numerical models must be produced to determine their mechanical behavior. Load bearing tissues in mammals are typically composed of collagenous fibrous networks connected by covalent cross links. To accurately model the behavior of these complicated tissues, a two dimensional Representative Volume Element has been formulated. The RVE utilizes truss elements, linear elastic springs and constraint forces to provide accurate behavior. The RVE behavior is calibrated to mimic experimental tensile testing of collagen gels by Xu et al. (International Journal of Biomaterials, 2011, pp. 1-12). The RVE behavior represented that of the experiments including producing a "J" shaped stress-strain curve and a brittle failure point of rupture. The simple truss structure RVE is simple enough to be utilized in multiscale finite element methods, while still describing accurate behavior of collagenous materials.

Acknowledgements:

I would like to thank Professor Franck Vernerey of the University of Colorado Civil Engineering Department. He has been an integral part of my learning process while obtaining my master's degree. Without him, the inspiration for my thesis topic would never have come to fruition. His help and encouragement has made my research an enjoyable feat.

I would also like to thank our entire research group led by Dr. Vernerey. The weekly collaboration of ideas between students is something that doesn't happen nearly enough. The advice and encouragement from peers can prove to be the most useful.

Contents

Introduction

Collagen based tissues are found in most load bearing organs of mammals. It is present in tendons, ligaments, bones, arteries and cartilage. [1] The field of tissue engineering often utilizes collagen as a scaffold for tissue grafts in various implants [2]. On the molecular level collagen is a hierarchal protein structure made of macromolecules. On the microscopic level collagen is a fiber reinforced composite whereby the orientation and organization of collagen greatly impacts the behavior of the tissue.
In connective tissue there are two types of reinforcing fibers: collagen and elastin. Collagen and elastin serve two different purposes in tissues. Collagen is strong and rigid in tension and helps to carry mechanical load. For example, the mechanical load in a stretched Achilles tendon is carried through tissue composed mainly of collagen. Elastin is the mechanism by which tissues return to their original shape. Elastin is responsible for skin returning to its original configuration when stretched. Of specific interest is the failure of collagenous fiber reinforced materials through fracture and crack propagation by means of fiber failure, and the effects of tissue properties on material behavior. [3].

The behavior of collagenous materials is highly dependent on the orientation of the collagen fibers, thereby making such materials anisotropic [4] [5]. The anisotropic micro-behavior of collagen must be accounted in the development of models mimicking the behavior of such tissues. Modeling the macro scale behavior of a fibrous tissue requires special constitutive and mechanical formulations which account for material anisotropy everywhere in the model. A multi-scale approach is proposed to efficiently model the bulk behavior of the material while capturing the micro behavior at a localized level. Multi-scale modeling methods try to capture the effects of microstructure on the macroscopic behavior of materials [5]. The scope of this research is to develop an efficient Representative Volume Element that captures the microstructure and behavior of a collagen fiber based tissue and to successfully initiate a failure mechanism on the micro scale. The RVE will then be implemented in a multi-scale finite element code and used to determine the fracture behavior of the material.

The proposed RVE will utilize truss elements to represent collagen fibrils. This assumption helps to provide computational efficiency to the model while still capturing the behavior of collagen. The RVE is modeled to allow for variability in material properties as well as variability in the anisotropy of the material. By adjusting the properties of the RVE, accurate material behavior can be compared to experimental tests of collagenous materials to calibrate the micro-model. Optimization of the structure may also be achieved to tailor the RVE for specific loading conditions.

Further calibration of the RVE is achieved by running benchmark tests. Benchmark tests will ensure that the RVE passes requirements for simple structural behavior. Further tests are presented for the RVE model and compared to experimental testing of collagenous gel networks to ensure the behavior of the RVE is accurate. Desirable behaviors in the RVE related to true collagen behavior include fiber realignment to the direction of the applied force and J-shaped stress strain relationships. After confirming the appropriate behavior of the RVE, a parametric analysis is run to analyze the behavior of a continuum subject to changing the properties of the RVE. The goal of the parametric analysis is to determine the geometric and material configuration of an RVE that has the highest fracture toughness by computing the J integral of the material. The fracture toughness of a material is arguably the most important property in designing for the failure of materials.

Literary Review

There has been much previous work on the modeling of collagenous tissues in literature. Of particular interest are the studies done by Agoram and Barocas 2001 [5], Klisch 1999 [4], Simha 1998 [6], and Lanir 1982 [7]. The work presented in this paper looks to improve upon the studies that have already been done on collagen based composites.

The inspiration of the research done within this paper is derived from the work of Agoram and Barocas. In their 2001 article they looked at the multiscale modeling of collagenous fiber networks. They developed a model in which the micro elements for multiscale formulation were made up of rigid fiber elements with crosslinks at intersections of fibers. The following research departs from Agoram and Barocas in the fact that their model of crosslinks introduced penalty elements connecting the ends of intersecting fibers. While this method of imposing cross link connections is effective, it makes implementing failure in crosslinks conceptually difficult, as the elongation of different penalty elements may be significantly different. This leads to the problem of which penalty elements to delete, and what effect this has on the cross link behavior [5]. This behavior is to be improved by treating cross links as single spring elements and penalizing fiber bending by enforcing fibers to remain parallel [5].

The work done by Klisch utilizes fiber reinforced continuum theory to model the behavior of collagen fibers within vertebrate disc tissues. While this method is both accurate and computationally inexpensive, it is only effective for tissues in which the collagen fiber orientations are prescribed. Fiber reinforced continuum theory requires that the orientation of fibers be known within the matrix. This is to be improved upon by creating a more general model in which tissues that have totally random collagen orientations as well as prescribed orientations may be implemented [4].

Simha considers modeling collagenous materials using composite theory. In this research, collagen fibrils were assumed to be cylinders restrained by an elastic matrix. The behavior of the material then becomes a function of fiber orientation and volume fraction. While these two parameters are certainly important to the behavior of collagenous tissues, they mask the major contribution of cross links [6].

The work done by Lanir develops a set of constitutive relations to model the behavior of collagen gels. These constitutive equations rely on the modeling of thin flexible fibers and an amorphous matrix providing resistance to fiber movement. Again this research does not include the addition of cross linking into the behavior of the collagenous material [7].

Structure and Mechanics of Collagen

More than two dozen types of collagen have been identified. Type I collagen is by far the most abundant, and is the focus of this research. Type I collagen is the basic building block in bones, tendons, ligaments, dentin, skin arteries and cartilage [1] [3]. The structure of Type I collagen tissue is hierarchal. On the molecular scale, collagen is made up of three polypeptide chains arranged in a left handed triple helix. Type I collagen is composed of two α1 polypeptide chains and one polypeptide α2 chain. α1 and α2 describe the amino acid sequence of the peptide chains that makeup collagen proteins [8]. Cross links between collagen proteins are formed between the ends helices through covalent bonds between amino terminals and carboxyl terminals of the triple helix.

Helical collagen molecules are on the order of 300nm long, and only a few nanometers wide. The collagen molecules are arranged in five segments linearly. Each collection of five collagen molecules is called a microfibril [1]. Microfibrils are the building blocks of collagen fibers. Cross links form between the first and fifth segments of the microfibrils via a covalent bond between the ends of each collagen molecule. These bonds arrange collagen fibrils into a staggered pattern. The staggered pattern of collagen microfibrils is evident in microscopic images of collagen in the form of striated bands.

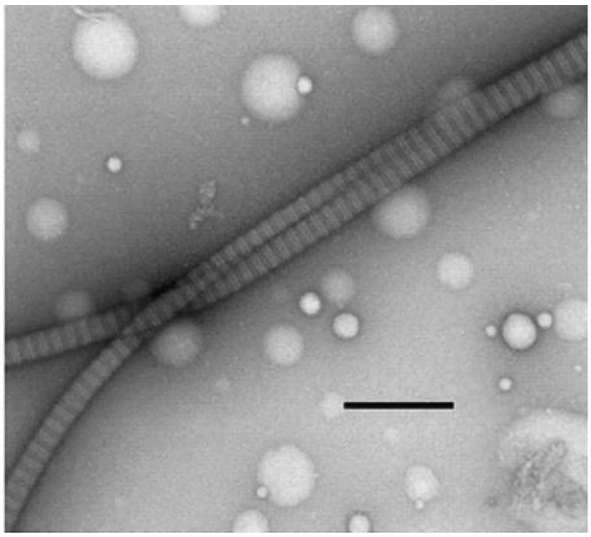

Figure 1: Striations in Collagen Microfibril. Image from Chapter 3 of Collagen Structure and Mechanics by P. Fratzl

The stagger distance forms gaps with length "D" based on the amino acids in the collagen peptide chains. For Type I collagen, D is typically 67 nm. Many collagen fibrils then pack themselves into collagen fibers. Collagen fibers are typically made up of hundreds of fibrils and can be 50 to 500 nm in diameter, and on the order of 100 microns long [3] [8] [9].

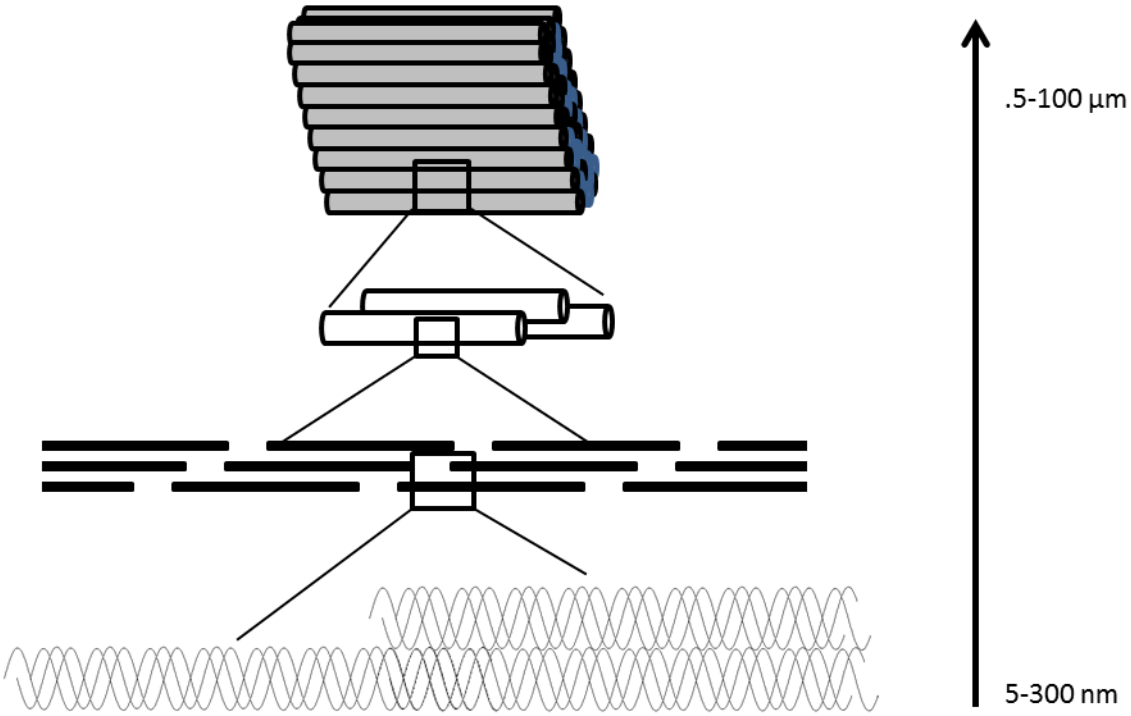

Figure 2: Hierarchal Structure of Collagen Fibers

The chemical makeup of collagen fibers allows for strong inter-fiber crosslinking. The inter-fiber crosslinking is the complex whereby collagenous tissues achieve their strength and stiffness. Methods of mimicking the crosslinking process are fully described in Barnard 1987.

Domain and Governing Mechanics of RVE

The physical domain of the RVE defined within this paper is a two dimensional rectangular element. The micro scale RVE of interest is composed of two different elements. The first element is a fiber element. The RVE is populated by randomly generated fibers with either prescribed fiber orientation or random fiber orientation [10]. Fiber elements are considered as truss elements within the RVE. Truss elements are bars that undergo deformation along the axis of the bar as well as a rotation in global space. Collagen fibers have a particularly high aspect ratio on the order of 100:1. Collagen fibers would be most accurately modeled as curved beam elements. Most Type I collagen fibers are not entirely straight and contain waviness. The waviness of collagen describes the amount of bending and twisting present in an individual collagen fiber. To fully capture the waviness and flexibility of collagen fibers, beam effects such as fiber curvature and buckling would need to be considered. Previous work has been done utilizing arbitrarily curved beam elements in Vernerey and Pak 2011. This model introduces complicated beam elements able to reproduce the behavior of collagen fibers in a network. Their research did not implement these curved beam elements into a real fibrous network and, and is beyond the scope of this research [11]. Modeling collagen fibers as truss elements forces the assumption that all fibers are modeled as linear elements, and that the linear elements carry no bending forces.

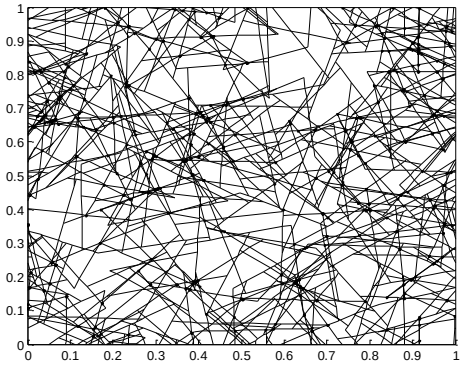

Figure 3: Proposed Domain of RVE

The second element in the RVE is a cross link element. Cross links form between collagen fibers through covalent bonds when fibers achieve a sufficient contact distance. Cross links are highly flexible bonds with minimal rotational stiffness [9]. The covalent bonds between collagen fibers are modeled as flexible linear springs with no rotational stiffness. The assumption of reduced rotational stiffness for cross links allows for a conceptually simpler model as well as increased computational efficiency. Cross links account for additional stiffness within the RVE and also allow fibers to slide and rotate amongst each other [12].

To numerically model the connection between cross links and fibers, the fibers themselves must be modeled as multiple truss elements. Subdividing fibers into multiples elements allows forces and displacements caused by cross links to be accounted for. The connection between the truss elements represent the location where the cross link is connected to another fiber, and is accounted for by introducing a node [5]. In normal two dimensional truss models, horizontal and vertical displacements at member ends must be restrained (as long as they are not zero force members). The modeling of randomly oriented fibers, and thereby truss members, poses a problem in the stability of the RVE structure. This inherent stability problem is solved by enforcing two assumptions. The first assumption is that all of the elements that make up a fiber remain collinear throughout deformation. This means that elements will not "kink" around a cross link intersection. This will also ensure that the individual elements do not

undergo any rotation through the length of the fiber. This assumption requires that a constraint force be placed on the elements. While in reality collagen fibers may undergo curvature, a kink in the fiber almost certainly means that the fiber has failed. Collinear elements prevent the fiber from having a kink and remove the potential numerical failure point at cross links. The second assumption that is made is that elements that are "hanging" off of the end of a fiber provide no addition to the mechanical behavior of the model. Following this assumption all hanging elements are subsequently removed from the model. Without the deletion of these elements from the model certain nodes would have no restraint from translational displacements and therefore yield an unstable structure.

To capture the fracture and failure of the RVE at a microscopic scale, the fibers and cross links are assumed to be perfectly brittle materials obeying Hooke's Law. The fiber elements will break when they reach a prescribed ultimate stress, and the cross links will break when they reach prescribed ultimate elongation.

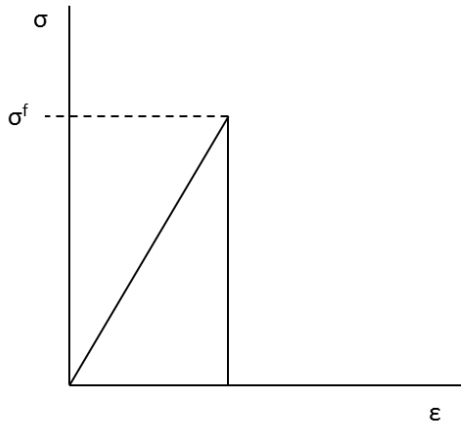

Figure 4: Stress Strain Curve for Linear Elastic/Brittle Material

The criterion of an ultimate elongation is based on the fact that cross links represent covalent bonds between collagen fibers. When the points of intersection between two fibers become sufficiently far apart, that covalent bond is destroyed, and the crosslink can no longer continue carrying any load. To increase the simplicity of the micro model, cross links are assumed to have stiffness only in translation modes. If two fibers undergo a relative rotation but no translation, the cross link will impose zero force on the associated fibers. The covalent bonds of crosslinks are physically much weaker than the bonds holding collagen fibers together. To model this behavior, the cross link spring stiffness is much lower than the axial stiffness of the collagen fibers [13]. This assumption allows the fibers to undergo large amounts of translation and rotation amongst one another without transferring excessive stress amongst fibers. This behavior mimics the untangling and realigning of collagen fibers that is seen in experimental testing of collagenous matrices.

The given RVE will follow periodicity rules at the boundaries of the element. For example, if a fiber ends on the left side on an element, there should also be a fiber that begins on the right side of the element with the same vertical coordinate and same slope as the original element.

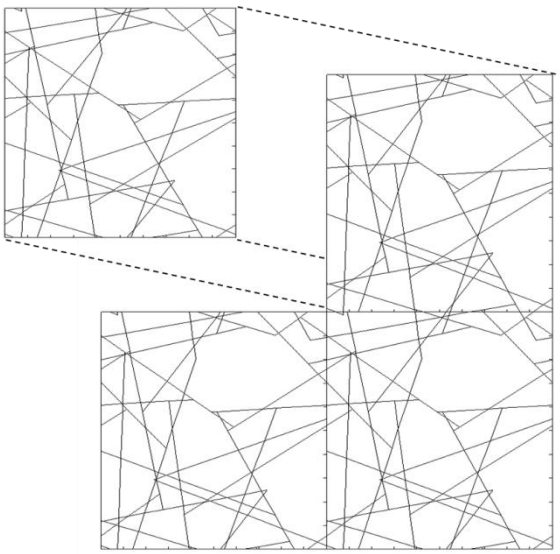

Figure 5: RVE Demonstrating Periodic Fibers on Boundaries

If two RVE's are stacked together, the fibers should look like they are running through the boundary of one RVE and continue flawlessly to the next element. By enforcing the element to be periodic, it can be used to replace any and all macro elements throughout the continuum model and maintain appropriate behavior [14].

In natural tissues and materials, the collagen fibers are usually under stress in vivo. Since collagen fibers prefer to be aligned in the direction of their applied force, collagen in vivo typically has a prescribed orientation. The orientation of collagen fibers is dependent on the state of stress of the material [3]. For example, the collagen fibers found in tendons are typically arranged parallel to one another in the direction of tendon stretching, while the collagen fibers in skin tissues are randomly oriented to carry stresses in multiple directions. Experimental collagenous gels typically have a random orientation of fibers [15], [16]. The following report will investigate both fixed orientation and randomly oriented collagen RVE's to understand how collagen alignment affects RVE behavior.

Realistic collagenous materials have a random attribution of properties. Each collagen fiber has a different strength, length and stiffness and will be treated as separate parameters within the analysis of the RVE [17]. It will be assumed that each property of each fiber will be based on a random normal distribution. For example, the average ultimate tensile strength of tendon tissue (which is at least 75% collagen by dry weight) given by Holzapfel (2000) is 50-100 Mpa. The normal distribution of fiber strength may then be described by the function:

$$f(x) = \frac{1}{\sqrt{2\pi\sigma^2}} e^{-\frac{(x-\mu)^2}{2\sigma^2}} \tag{1}$$

Each property is described by two variables: σ Is the variance of the property and μ is the mean or expected value of the property [17]. For example, a single fiber in a large set of fibers with mean tensile strength of 50 Mpa and a variance of 100 Mpa will have a 4% chance of having a tensile strength of 50 Mpa, as can be seen in the below figure.

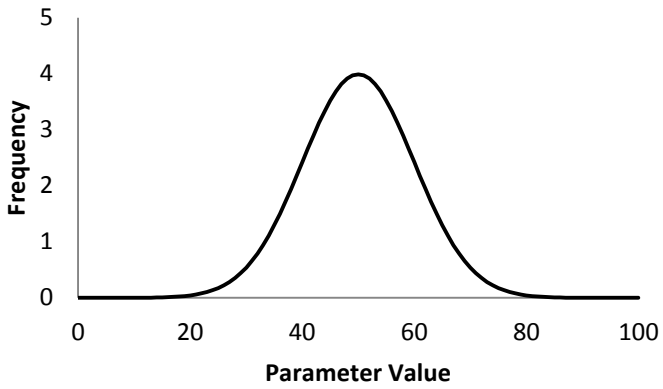

Figure 6: Normal Distribution of RVE Parameter

The orientation of fibers will be determined by a predefined value of anisotropy, zeta. This value will allow completely random, or perfectly oriented fibers, or anywhere between to be defined. The RVE will be able to model up to four different predefined fiber directions. If zeta is zero, all of the fibers within the RVE will have the one of the orientations defined by the user. If zeta is one, then all of the fibers will have a completely random orientation. If zeta is between zero and one, the fiber orientations will tend around the prescribed value, but their angles will differ slightly. The figure below shows RVE's for different zeta values. The number of fibers for each RVE is 100, and the average length of fibers is one half the length of the RVE. As zeta increases, the orientation of the fibers becomes more random.

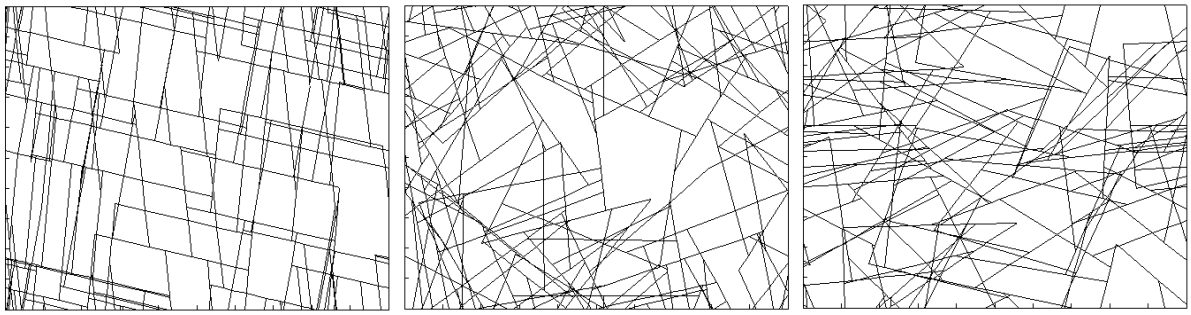

Figure 7: a) zeta = 0. b) zeta = 0.5. c) zeta = 1.0

RVE Development

The formulation of truss elements representing fibers is derived from one dimensional bar elements. A bar element has two nodes, one on each end. Each node contains one degree of freedom; a translation in the direction of the axis of the bar. Bar elements are translated into global space through a rotation matrix to obtain truss elements. The rotation matrix converts the end displacements of a bar into x and y displacements in global space. Bar elements are developed following three assumptions: that the strain within the element is constant along its length, the cross sectional area and Young's Modulus remain constant along the element's length, and the strain in the element is related to the stress via Hooke's Law. Bar elements will be represented by two nodes with one degree of freedom each. The three equations that define the mechanics of the problem are the constitutive equation (2), strain-displacement relationship (4) and force balance (5).

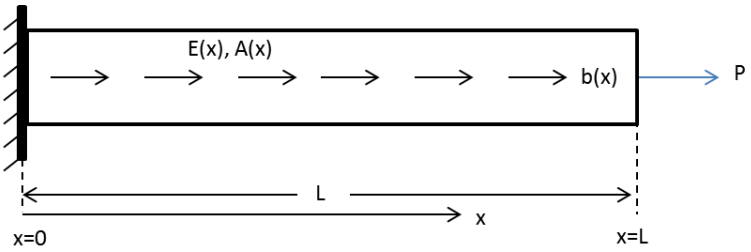

Figure 8: Representative Bar Test Element

The stress-strain relationship in Equation 2 for the bar element is assumed to be perfectly elastic and brittle. Each bar element will follow Hooke's Law, behaving linearly until it reaches a brittle failure stress criteria. If a bar exceeds its failure criterion the Young's Modulus, or material stiffness of the element drops nearly to zero. The strain-displacement relationship relates the gradient of displacement of an element to the strain within the element. The focus of this study assumes that the gradient of displacement is a constant function of the end displacements of the element. Therefore, each truss element will have a constant strain along its length. The following finite element formulation is based off of the formulations derived from principals of virtual work presented by Szabo and Babuska 1991 as well as David Roylance 2001 [18], [19].

$$\sigma(x) = E\epsilon(x) \tag{2}$$

$$F(x) = \sigma(x)A \tag{3}$$

$$\varepsilon(x) = \frac{\partial u}{\partial x} \tag{4}$$

$$\Sigma F = F(x + \Delta x) - F(x) + b(x)A(x)\Delta x = 0 \tag{5}$$

Equation 5 describes the equilibrium of the element in which the sum of the forces along the bar is equal to zero. If Equation 5 is divided by Δx and the limit of Δx approaches zero, Equation 6 is generated.

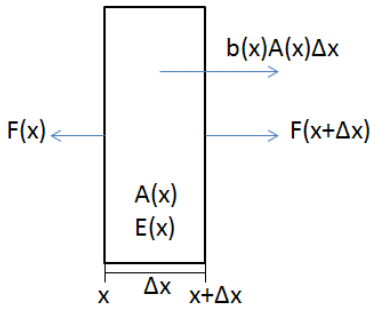

Figure 9: Equilibrium of Finite Slice of Bar Element

If Equations 2, 3, and 4 are substituted into Equation 6 the strong form of the bar formulation is obtained in Equation 7.

$$\frac{dF}{dx} + bA = 0 \tag{6}$$

$$\frac{d}{dx}\left(EA\frac{du}{dx}\right) + bA = 0, 0 < x < L \tag{7}$$

The Finite Element Method (FEM) provides a mathematical process of solving differential equations resulting from structural analysis. The FEM massages complicated differential equations (Strong Form) into integral form (weak form), and then discretizes the domain in order to implement numerical integration (Finite Element Form). The strong form of the bar formulation in Equation 7 is the starting point in the finite element formulation for truss elements. Equation 7 must be transformed into the weak form in order to implement the FEM.

To go from the strong form to the weak form, the strong form of Equation 7 is multiplied by an arbitrary weighting function w and written in integral form in Equation 8. The weighting function w is assumed to be valid along the entire domain of the element. Equation 8 can then be integrated by parts to generate Equation 9.

$$\int_0^L \left(\frac{dF}{dx} + bA\right) w dx = 0 \tag{8}$$

$$(Fw)\Big|_0^L - \int_0^L \left(F\frac{dw}{dx} - bAw\right) dx = 0 \tag{9}$$

The stress at x=L of the test element is zero, since the applied force at the end of the element is also equal to zero. The test function w at x=0 of the element is also equal to zero, as it is a fixed boundary condition. These conditions yield the complete weak formulation for a bar element in one dimension.

$$\int_0^L \left(EA\frac{du}{dx}\frac{dw}{dx} - bA\right) dx = F(L)w(L) \tag{10}$$

To go from the weak formulation to the finite element formulation, the domain of $0 \rightarrow L$ is discretized into elements of finite length. The discretization of a truss element requires that values of displacements u, and weighting function w be defined at the nodes of discretized elements. This yields a vector of nodal displacements and nodal values of w.

$$\boldsymbol{u} = \begin{Bmatrix} u_1 \\ u_2 \\ . \\ . \\ . \\ u_i \\ . \\ . \\ u_n \end{Bmatrix} \quad \boldsymbol{w} = \begin{Bmatrix} w_1 \\ w_2 \\ . \\ . \\ . \\ w_i \\ . \\ . \\ w \end{Bmatrix} \tag{11}$$

The values for displacement u and weighting function w are still desired along the length of each discretized element. The values of w and u are linearly interpolated along the element using shape functions.

$$u(x) = N_1(x) + N_2(x) \tag{12}$$

In the case of a two node linear bar element there are two shape functions, one for each node. The shape function for node "i" of a given element is defined to be equal to unity at the coordinates of node "i" and zero at the coordinates of node "j". This ensures that the value of displacement at a given node is equal to the displacement at that node. The shape functions for an n node element are given below.

$$N_J(x) = \prod_{\substack{i=1 \\ i=j}}^{n+1} \frac{x - x_i}{x_j - x_i} \tag{13}$$

In the case of a two node bar element, the two shape functions are given as:

$$N_1 = \frac{x-x_2}{x_1-x_2} \; N_2 = \frac{x-x_1}{x_2-x_1} \tag{14}$$

Shape functions must be used in order to interpolate the displacements along every discretized element. As systems become more complicated and more elements are defined, computing individual shape functions for each element becomes time consuming. To expedite the process of computing shape functions for elements, a parent element is defined. A parent element has fixed local coordinates and can be used to model any element within the domain. The introduction of a parent element makes for integration over individual elements the same no matter the geometry of the element.

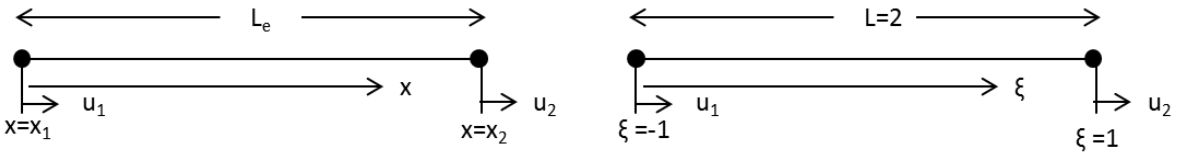

Figure 10: Physical and Parent Bar Elements

For a two node parent element, the shape functions may then be defined as in Equation 15. The shape functions of the parent, as well as the displacements at parent element nodes may be written in vector form as in Equation 16. Multiplying the shape function vector with the nodal displacement vector yields Equation 17, defining the scalar displacements along the element.

$$N_1 = \frac{1-\xi}{2} \; N_2 = \frac{\xi+1}{2} \tag{15}$$

$$\boldsymbol{N}(\xi) = [N_1 \quad N_2], \; \boldsymbol{u^e} = \begin{Bmatrix} u_1 \\ u_2 \end{Bmatrix} \tag{16}$$

$$u(\xi) = \boldsymbol{N}\boldsymbol{u^e} \tag{17}$$

In order to move between physical element and parent element coordinates, mapping functions must be defined. Mapping functions convert the coordinates from a physical to a parent element or vice versa. The mapping and inverse mapping functions for a two node bar element are listed below. With the mapping functions defined, the derivative of the displacement vector $\mathbf{u}^e$ may now be obtained via the chain rule. The derivative of the shape function vector as shown in Equation 20 is defined as the $\underline{\mathbf{B}}$ matrix.

$$x(\xi) = \frac{x_1+x_2}{2} + \frac{x_2 - x_1}{2}\xi \tag{18}$$

$$\xi(x) = \frac{2}{x_2 - x_1}x - \frac{x_1 + x_2}{x_2 - x_1} \tag{19}$$

$$\frac{du}{dx} = \boldsymbol{B}\,\boldsymbol{u}^e \tag{20}$$

$$\boldsymbol{B} = \left[\frac{\partial N_1}{\partial \xi} \quad \frac{\partial N_2}{\partial \xi}\right]$$

After discretizing a bar into finite elements, the integral over the entire domain in the weak form becomes an explicit summation of integrals over finite element domains in Equation 21. The derivatives over the individual elements may be written in terms of the **B** matrix times the nodal values of displacements and weighting functions, $\mathbf{u}^e$ and $\mathbf{w}^e$. The values of the weighting function along the element may be written as the shape functions **N** times the nodal values of the weighting functions $\mathbf{w}^e$. The weak form is then rewritten as in Equation 22. The weighting values in $\mathbf{w}^e$ are constant along the length of each element. Therefore they may be pulled out to the front of the integral of each element. Equation 22 is then rewritten in three parts: an internal strain energy part, an external energy part due to body forces, and an external energy part due to traction forces.

$$\sum_{e=1}^{n_e}\int_{\Omega_e}\left(EA\frac{du}{dx}\frac{dw}{dx} - bAw\right)dx - Pw(L) = 0 \tag{21}$$

$$\sum_{e=1}^{n_e}\int_{\Omega_e} EA(\boldsymbol{B}\,\boldsymbol{w}^e)(\boldsymbol{B}\,\boldsymbol{u}^e) - bA\boldsymbol{N}\,\boldsymbol{w}dx - Pw(L) = 0 \tag{22}$$

$$\sum_{e=1}^{n_e}\left(\underbrace{-\underline{\boldsymbol{w}}^{\boldsymbol{eT}}\int_{\Omega_e}\left[EA\,\underline{\boldsymbol{B}}^{\boldsymbol{T}}\underline{\boldsymbol{B}}dx\right]\underline{\boldsymbol{u}}^{\boldsymbol{e}}}_{Internal\ Strain} \underbrace{-\ \underline{\boldsymbol{w}}^{\boldsymbol{eT}}\int_{\Omega_e} bA\underline{\boldsymbol{N}}^{\boldsymbol{T}}dx}_{Body\ Force}\right) \underbrace{-\ Pw(L)}_{Traction} = 0 \tag{23}$$

The internal strain energy tem may be rewritten in terms of an element stiffness matrix multiplied by the nodal displacements. The body force energy term may be rewritten in terms of an external force vector, while the traction term may be rewritten in terms of a prescribed external force at boundary nodes. The weak form is rewritten in Equation 24.

$$\sum_{e=1}^{n_e}\left(-\underline{\boldsymbol{w}}^{eT}\left[\underline{\underline{\hat{\boldsymbol{k}}}}^{e}\,\underline{\boldsymbol{u}}^{e}-\underline{\hat{\boldsymbol{f}}}^{e}_{\boldsymbol{bext}}\right]\right)-\underline{\boldsymbol{w}}^{T}\underline{\boldsymbol{f}}_{\boldsymbol{text}}=0 \tag{24}$$

$$\hat{\boldsymbol{k}}^{e}=\int_{e}EA\boldsymbol{B}^{T}\boldsymbol{B}dx \tag{25}$$

$$\hat{\boldsymbol{f}}^{e}_{\boldsymbol{bext}}=\int_{e}bA\boldsymbol{N}^{T}dx \tag{26}$$

In order to convert the bar element into a truss element, the element stiffness matrix and body force vectors must be translated into global space. To do this, a transformation matrix is constructed. The individual cells of the transformation matrix use the angle between the local element axes with the global x-axis. Once the element stiffness matrices and body force vectors have successfully been transformed, they may be assembled into global stiffness matrices and global force vectors. The assembly of all elements into global matrices and vectors yields the finite element formulation for truss elements.

$$\boldsymbol{T}=\begin{bmatrix}\cos\theta & \sin\theta & 0 & 0\\ 0 & 0 & \cos\theta & \sin\theta\end{bmatrix} \tag{27}$$

$$\boldsymbol{k}=\boldsymbol{T}^{T}*\hat{\boldsymbol{k}}_{e}*\boldsymbol{T} \tag{28}$$

$$\boldsymbol{f}^{e}_{\boldsymbol{bext}}=\boldsymbol{T}^{T}*\hat{\boldsymbol{f}}^{e}_{\boldsymbol{bext}} \tag{29}$$

$$\boldsymbol{K}=\bigwedge_{e=1}^{n}\boldsymbol{k}_{e} \tag{30}$$

$$\boldsymbol{f}_{ext}=\bigwedge_{e=1}^{n}(\boldsymbol{f}^{e}_{\boldsymbol{bext}})+\boldsymbol{f}_{\boldsymbol{text}} \tag{31}$$

$$\boldsymbol{K}*\boldsymbol{u}=\boldsymbol{f}_{ext} \tag{32}$$

The size of the global stiffness matrix **K** is [ndof,ndof] where ndof is the number of degrees of freedom for the system. In the system of interest, the displacement vector **u** represents the vector of unknown nodal displacements. The local element stiffness matrix for a cross link element is given by Equation 33. Since the cross links are assumed to be linear springs, their stiffness matrix is a simple function of spring constants and element orientations.

$$E_x\begin{bmatrix}c^2 & sc & -c^2 & -sc\\ sc & s^2 & -sc & -s^2\\ -c^2 & -sc & c^2 & sc\\ -sc & -s^2 & sc & s^2\end{bmatrix} \tag{33}$$

s=sinθ and c=sinθ

Again the angle θ represents the angle between local and global coordinate systems for each element. The above stiffness term is decomposed into appropriate degrees of freedom and added into the correct

locations of the global stiffness matrix **K**. The global stiffness matrix that is derived from the finite element formulation is singular as given. Boundary conditions must be applied to the system in order to ensure a determinate stiffness matrix. Boundary conditions will be discussed in a later section.

The assumption that all elements along the length of a fiber remain parallel is enforced by introducing Lagrangian multipliers to the system. Lagrangian multipliers work like additional forces imposed on certain degrees of freedom to enforce desirable motion. In the case of co-linear elements, constraints are placed on degrees of freedom that are either associated with an intersection node, or nodes adjacent to intersection nodes. These constraints come from the assumption that if elements within a fiber are parallel, and that the connectivity between adjacent elements is maintained, that the elements remain collinear. The introduction of Lagrangian multipliers is introduced into the system in Equation 39.

$$\begin{bmatrix} \boldsymbol{K} + \boldsymbol{\lambda H} & \boldsymbol{G}^T \\ \boldsymbol{G} & \boldsymbol{0} \end{bmatrix} \begin{Bmatrix} \boldsymbol{u} \\ \boldsymbol{\lambda} \end{Bmatrix} = \begin{Bmatrix} \boldsymbol{f} - \boldsymbol{G}^T \boldsymbol{\lambda} \\ -\boldsymbol{g} \end{Bmatrix} \tag{34}$$

In the above system $\boldsymbol{\lambda}$ introduces a vector of new degrees of freedom, while **g** represents the constraint equations introduced by the enforcement of parallel fibers. **G** and **H** represent the first and second differentials of g respectively. The constraint forces represented in g are derived in Equations 41-44 from the assumption that parallel fibers maintain the same slope.

$$m_1 = \frac{(y_2 + v_2) - (y_1 + v_1)}{(x_2 + u_2) - (x_1 + u_1)} \tag{35}$$

$$m_2 = \frac{(y_3 + v_3) - (y_2 + v_2)}{(x_3 + u_3) - (x_2 + u_2)} \tag{36}$$

$$m_1 = m_2 \tag{37}$$

$$\begin{aligned} \boldsymbol{g} = (y_2 + v_2 - y_1 - v_1) * (x_3 + u_3 - x_2 - u_2) \\ - (y_3 + v_3 - y_2 - v_2) * (x_2 + u_2 - x_1 - u_1) \end{aligned} \tag{38}$$

By definition each intersection node will have a constraint applied to it. In the above equations, x_i and y_i represent nodal coordinates of intersection nodes and surrounding nodes. Variables u_i and v_i represent the displacements of the degrees of freedom corresponding to said nodes. **G** becomes a row vector defined as the partial derivative of **g** with respect to each degree of freedom. Since g has only six values that vary with respect to degrees of freedom, each row of **G** will have only six non-zero values.

$$\boldsymbol{G}_i = \frac{d\boldsymbol{g}}{d\boldsymbol{u}_i} \tag{39}$$

The second derivatives in the **H** matrix all drop to zero since **g** contains linear functions of degrees of freedom **u**. The introduction of the Lagrangian constraints into the mathematical formulation of the problem produces a geometric nonlinearity in the system. The geometric nonlinearity comes from the dependency of the stiffness matrix **K** on nodal displacements **u**. In order to deal with the geometric nonlinearity, Newton Raphson iteration is introduced. Newton Raphson iteration utilizes the derivative of a function and a prescribed "time step" in order to converge on the appropriate root of a function. In the case of this problem, the internal energy of the system is to be minimized. The equation to be minimized by the Newton Raphson method is shown in Equation 40. The internal force of the system is equal to the internal strain force computed in Equation 23.

$$\boldsymbol{r} = \boldsymbol{F}_{int} - \boldsymbol{F}_{ext} \tag{40}$$

$$\boldsymbol{K}_{aug} = \begin{bmatrix} \boldsymbol{K} + \boldsymbol{\lambda H} & \boldsymbol{G}^T \\ \boldsymbol{G} & \boldsymbol{0} \end{bmatrix}, \boldsymbol{\Delta u} = \begin{Bmatrix} \boldsymbol{\Delta u} \\ \boldsymbol{\Delta \lambda} \end{Bmatrix} \tag{41}$$

$$\begin{gathered} When\ \boldsymbol{F}_{ext} = 0 \\ \boldsymbol{r} = \boldsymbol{K}_{aug} \boldsymbol{\Delta u} \end{gathered} \tag{42}$$

The residual r represents the additional internal energy that is left in the system from the constraint forces. After applying an initial displacement to the system, fibers will have kinks among the internal elements. The constraint forces applied to the system will try to straighten the kinks at each successive step of displacement. As the fibers get closer to being straight, the force correcting the fibers gets smaller, and therefore the residual force in the system becomes smaller. The Newton Raphson iteration slowly corrects the error in the orientation of the fibers until their orientation causes a minimum in the residual calculation, or in other words the residual approaches zero.

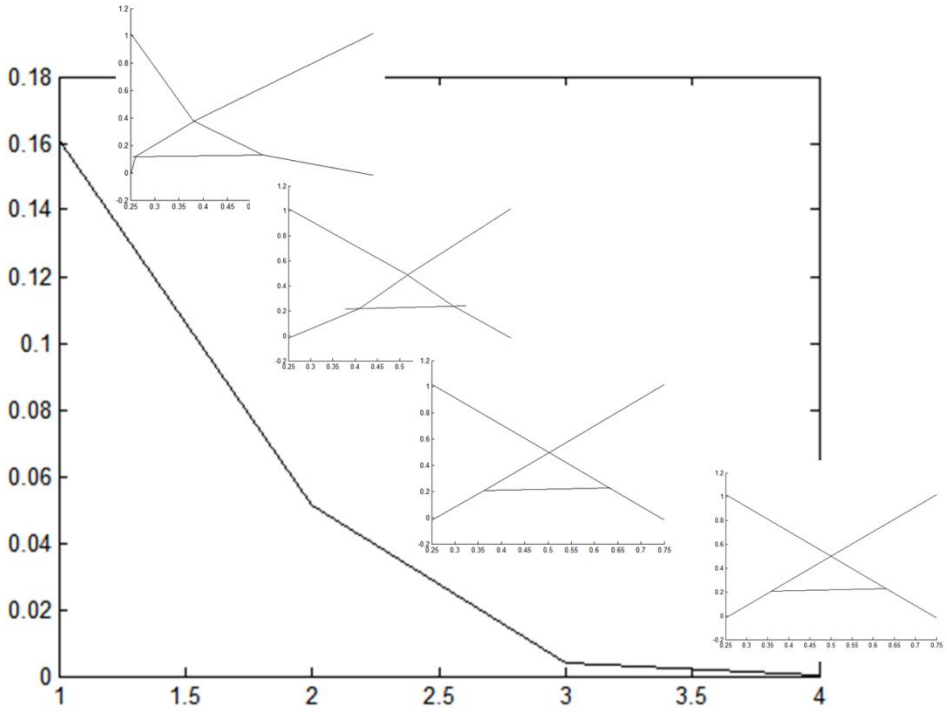

Figure 11: Convergence of Residual and Straightening of Fibers in Newton Raphson Iteration

In order to fully solve the system in Equation 46, the augmented stiffness matrix needs to be made determinate. This is achieved by imposing sufficient boundary conditions on the system. This is achieved by adding fixities at appropriate degrees of freedom so as to prevent all rigid body translations and rotations in the system. The process of applying boundary conditions is shown in Equation 43.

$$for\ DOF\ n\colon\ K_{n,i\neq n} = 0, K_{n,n} = 1, u_n = \Delta_n \tag{43}$$

With the appropriate boundary conditions applied, the incremental displacements imposed by the Newton Raphson iteration may be solved by inverting the augmented stiffness matrix and multiplying it by the residual. This will yield an incremental displacement value which can be used to update the constraint

forces, and recalculate the residual. The recalculated residual is used again to solve for an incremental displacement and the process is repeated until r is sufficiently close to zero. The final displacement of the system is the sum of the incremental displacements.

Failure in the analysis is predicted by applying total displacements in a discrete set of smaller increments. This allows for the stresses in fibers and elongations in cross links to be checked at each step of displacement. Stepping through the displacement of the RVE also allows for the global element stiffness matrix to be updated including displaced geometry. By updating element geometry information, nonlinear geometric behavior and failure can be successfully captured in the model.

Finite Element Implementation

The above finite element formulation was implemented in a series of Matlab programs. The main Matlab program that runs the simulation is called Fiber_FEM.m. Fiber_FEM initiates the formulation of a fiber reinforced composite problem, defines the discretization of elements and solves the mesh for unknown displacements. A flow chart of the computation process for the finite element implementation is shown below.

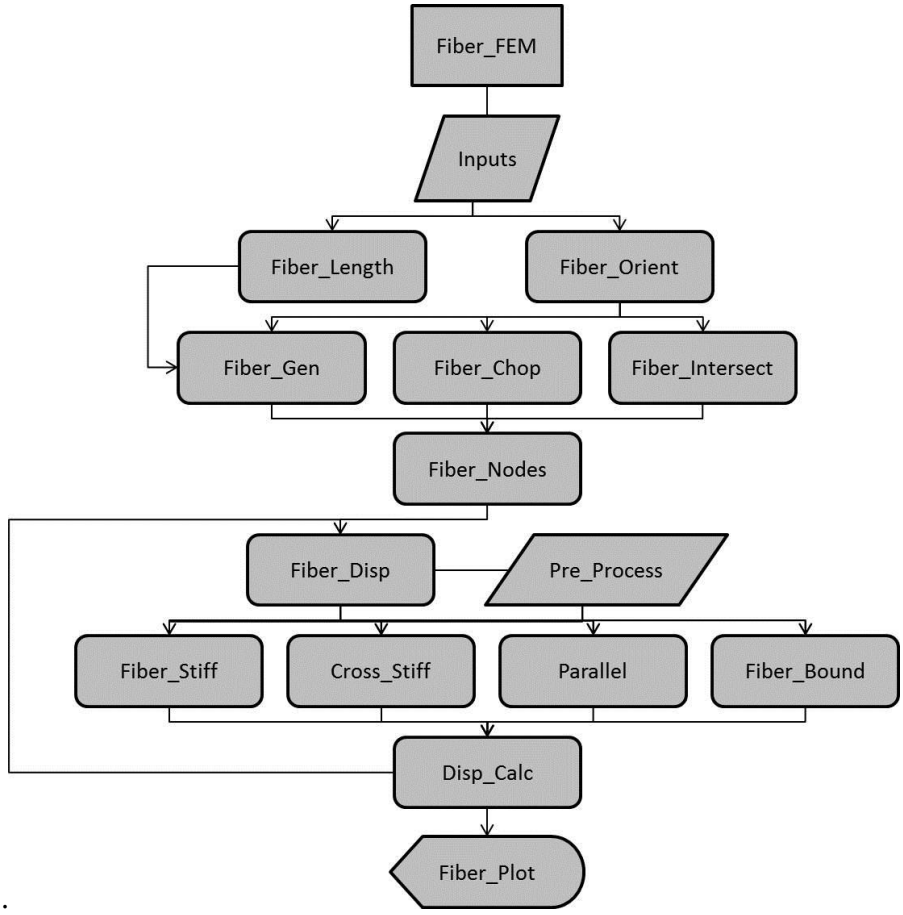

Figure 12: Flow Chart of Finite Element Code

After the program is initiated by Fiber_FEM, preprocessing is started when the program calls Inputs.m. The Inputs file provides a place for the user to define the properties of the system. Parameters such as RVE size, fiber number, fiber length, anisotropy factor and material properties are all defined in Inputs.m. After defining the properties of the simulation, Fiber_Length.m is called. Fiber_Length.m creates a vector of fiber lengths that follow a random normal distribution around the mean fiber length defined by the inputs. After the lengths of the fibers are defined, the orientation of the fibers is given within Fiber_Orient.m. The orientation of the fibers relies on the number of fiber directions and anisotropy factor to create a vector of fiber angles θ. The anisotropy factor is a factor that ranges from zero to one defined by the user. If the factor is zero, the fibers have a strict alignment as previously defined by the user. As the factor increases, the angles of the fibers can stray away from their strict alignment.

After the fiber information is defined, Fiber_Gen is used to create nodal coordinate information for the fibers. Fiber_Gen first creates a random distribution of seed points that act as the origin of each fiber.

The fibers are then grown from the seed points by adding half of the length along the orientation of the fiber and subtracting half of the length along the orientation of the fiber from the seed coordinates. This gives the start and end nodes of each fiber, as shown below.

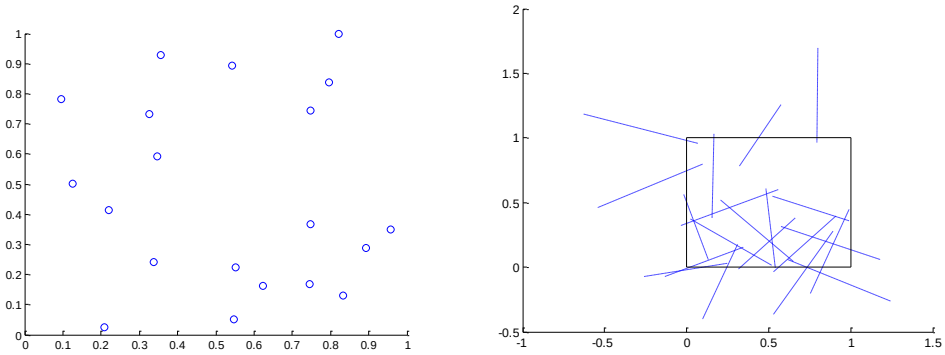

a b

Figure 13: a) Seed Points for Fibers. b) Generated Fibers

If the fiber length that has been defined is sufficiently long enough, fibers may have start or end nodes, or both defined outside of the RVE. These fibers must be cut, with their remaining sections periodically added to the other side of the RVE. This is achieved in Fiber_Chop.m. Fiber_Chop.m detects fiber nodes that are outside of the RVE boundary. The program then cuts these nodes and adds the fiber to the other side of the RVE.

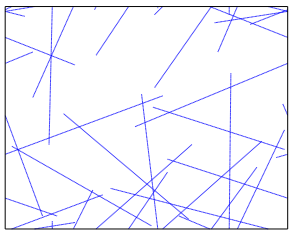

Figure 14: Fibers Cut Periodically at Boundaries of RVE

After the RVE has been made periodic, the cross links need to be introduced into the system. The cross links are assumed to be found anywhere two fibers intersect within the RVE. Fiber_Intersect.m determines the intersections of the nodes by comparing each fiber with all other fibers. By definition, if the cross product of two vectors defining two fibers is zero, then the two fibers are not parallel, and an intersection is possible. If the dot product of the vectors is greater than zero, but less than the square of the length of the fibers, then an intersection between the fibers exists. The coordinates of the intersections are saved and used to further define nodes of the system.

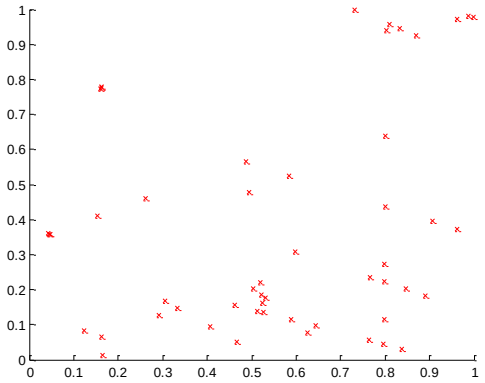

Figure 15: Intersections of Fibers

After the intersections of fibers have been defined, the nodal information and connectivity of the system is created. This is done within Fiber_Nodes. Fiber_Nodes achieves five things:

1. The coordinates of end nodes of each element making up a fiber is defined in a matrix. A fiber is split up into multiple elements if there are multiple intersections along the fiber. Therefore, all fiber ends as well as intersection points are given nodal coordinate values.
2. An element connectivity matrix is defined. This matrix stores information as to which node numbers are associated to the start and end of each element.
3. A cross link connectivity matrix is defined. The cross link connectivity matrix defines which node numbers are associated with the start and end of each cross link. By definition, all of the nodes within the cross link connectivity matrix must be intersection nodes.
4. "Lonely" nodes are deleted from the system, as well as the element connecting said node. A lonely node is defined as a node that is only connected to one element within the RVE, and is not fixed by boundary conditions. If this node and its element are not deleted, the system becomes unstable as all rigid body motions would not be restrained.
5. The intersections which are surrounded by two nodes are kept track of. If a node is sandwiched between two elements it is considered an "internal" intersection. Internal intersections are the nodes which parallel line constraints are applied to further in the formulation.

Fiber_Nodes.m completely defines the discretized RVE and ends the preprocessing of the system.

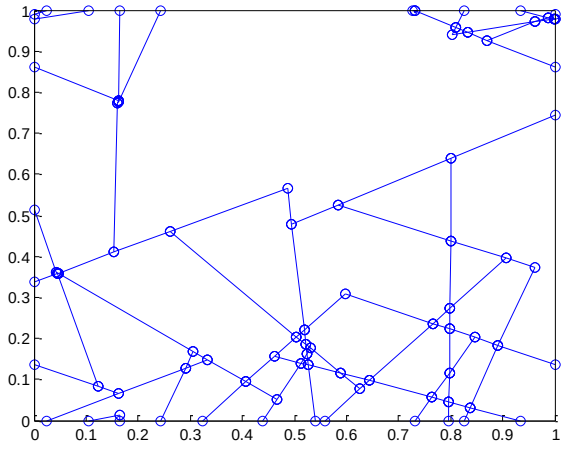

Figure 16: Fully Discretized RVE Domain

Once preprocessing is complete, the finite element formulations may be implemented. The formulation of element stiffness matrices, cross link stiffness matrices, internal force vectors and parallel line constraints are all produced within Fiber_Disp.m. Fiber_Disp.m also assembles all stiffness and force information into global matrices and vectors. The first file that Fiber_Disp.m utilizes is Fiber_Stiff.m. Fiber_Stiff.m utilizes the preprocessed information to define element stiffness matrices and assemble them into a global stiffness matrix, as defined by Equations 30 and 32. Cross_Stiff.m defines cross link stiffness matrices and assembles them into the predefined global stiffness matrix. After element stiffnesses are defined, the parallel fiber constraints are implemented within Parallel.m. Parallel.m utilizes Equations 34-39 to create an augmented stiffness matrix as well as constraint forces. Boundary conditions are then applied within Fiber_Bound.m as per Equation 43.

Once the augmented global stiffness matrix has been defined and properly fixed, the incremental displacement of the system can be solved for. Given the incremental displacement, and stiffness of the system, the internal force vector, or residual is calculated. If the norm of the internal force vector is large, then the residual of the linearized equation for solving the nonlinear system is also large. If the residual is not sufficiently close to zero, the constraint equations are updated to include the new nodal coordinates and displacements and the system is resolved. This process is repeated until the residual converges to a value sufficiently close to zero, representing that all fibers have been successfully made parallel.

After the residual successfully converges, the displaced shape of the structure for that given force or applied displacement has been found. The above process is then repeated for multiple steps of force or displacement. This is what is done to run a failure analysis of fibers and cross links. A total displacement is defined for the system. The total displacement is broken up into a sum of smaller displacements. After the solution for each small displacement is found, the internal stresses in the fiber elements and elongations of the cross links are computed. If either of these values exceeds their failure criterion, then the proper element is deleted from the analysis by a reduction of stiffness for said element. The simulation is then continued with the reduced element until all displacement steps have been simulated.

Benchmark Tests

Benchmark tests are conducted to prove the validity of the finite element code that has been introduced. Benchmark tests are tests in which either the closed form solution is easily found, or the solution is mathematically obvious. Here, two benchmark tests are provided to test assumptions made within the finite element coding.

Test Problem 1:
The first benchmark test is used to establish the validity in the assumption that the individual elements within a fiber remain parallel as forces are applied at intersections. In the first plot, there is an applied displacement in the negative x direction on the left side, and an applied displacement in the positive x direction on the right side. Without the constraint forces that are applied to the system, the vertical fiber would displace to have a kink in it (in fact this system would be unstable without parallel line constraints). The second plot shows the deformed shape of the system, and that the vertical fiber has maintained its straight orientation. The implementation of parallel line constraints holds valid, as there are no kinks present along fibers.

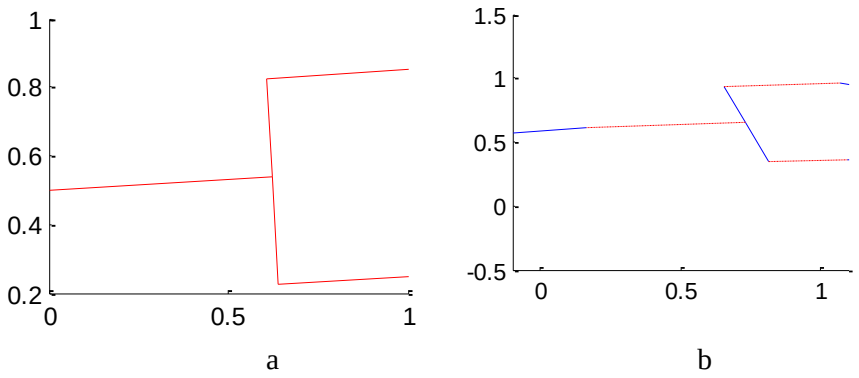

Figure 17: a) Straight Fiber Benchmark b) Displaced Benchmark

Test Problem 2:
Crosslinks within the RVE are assumed to be very flexible and must break after a defined amount of elongation. The first plot shows an RVE in which there is an applied displacement in the positive x direction on the right side of the RVE. The top and bottom nodes of the vertical fiber are each fixed. Since both nodes of this fiber are fixed, and parallel line constraints are enforced, this fiber should remain rigidly in its given position. The second plot shows the RVE with a small amount of applied displacement. The horizontal fibers are pulled to the right to stretch out the cross links connected to the rigid fiber. As a reminder, the only connections between fibers are achieved through cross link elements. The second plot shows the deformed cross links that have not yet reached their critical elongation value. The third plot shows the RVE at the next step in displacement. In this plot both cross links have elongated beyond their critical elongation value, and are therefore "deleted" from the model. To ensure that the model remains structurally stable, elements which have been "deleted" only experience a reduced stiffness value. This allows further steps of force or displacement to be imposed on the system.

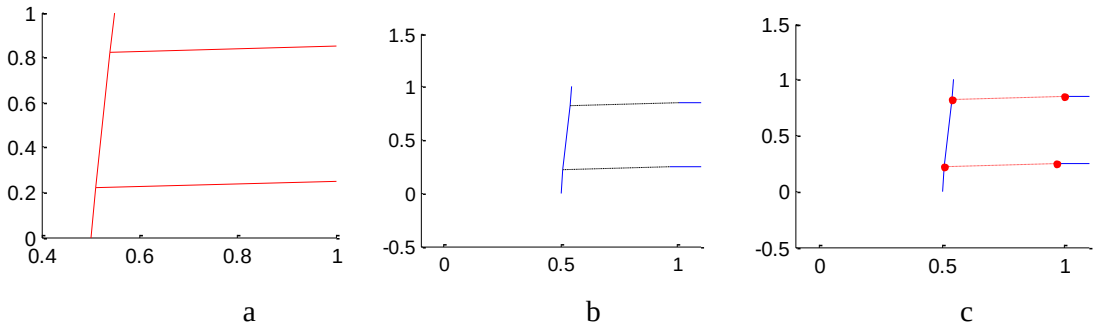

Figure 18: a) Cross Link Benchmark Test b) Displaced Unbroken Cross Links c) Broken Cross Links

Results

Literature provides that one of the key parameters in the behavior of collagen materials is cross link density [2], [3], [1]. The proposed code was used to determine the parameters that affected cross link density the most. It can be shown that as the number of fibers increases, the average length of fibers increases and the anisotropy of the collagen fibers decreases (increase in randomness in the RVE), the cross link density also increases. Fiber number and length both have a nonlinear effect on cross link density. The anisotropy value affects the cross link density asymptotically.

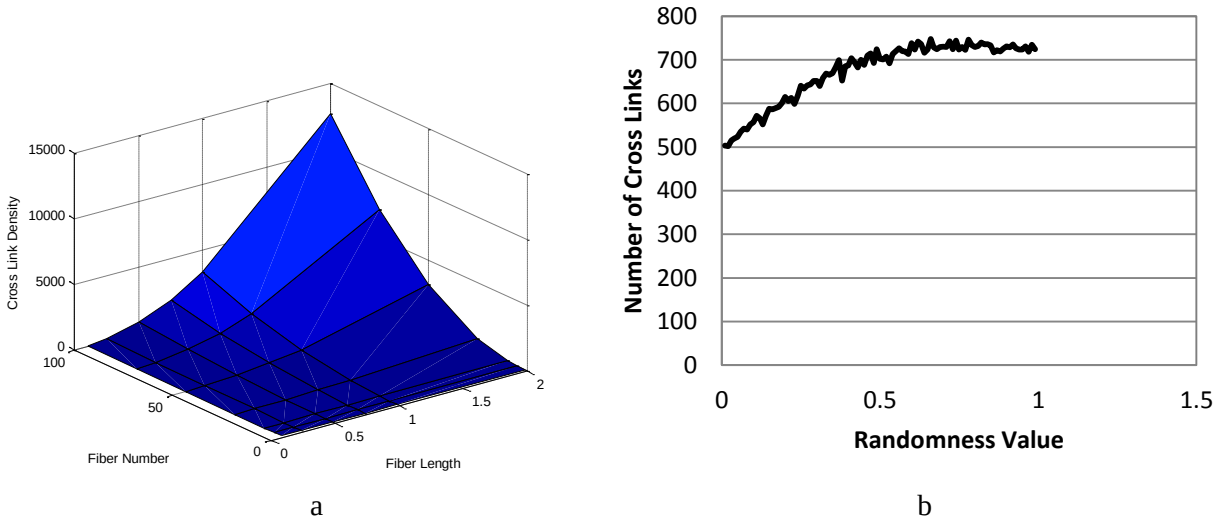

a b

Figure 19: a) Cross Link Density as a Function of Fiber Number and Average Fiber Length. b) Cross Link Density as a Function of Anisotropy

These plots prove what intuitive results one would expect. More fibers with longer length have a greater chance at intersecting one another, thereby creating more cross links. A material that is completely anisotropic has defined fiber orientations. This means that many fibers are parallel to each other, making cross linking much less likely. A material that has totally random fiber orientations will experience more cross linking as each fiber has a greater chance at potentially intersecting another fiber. The cross links also play a direct role in the stress strain response of the RVE. Below is an example of how increasing the stiffness of cross links also increases the tangent modulus of the RVE.

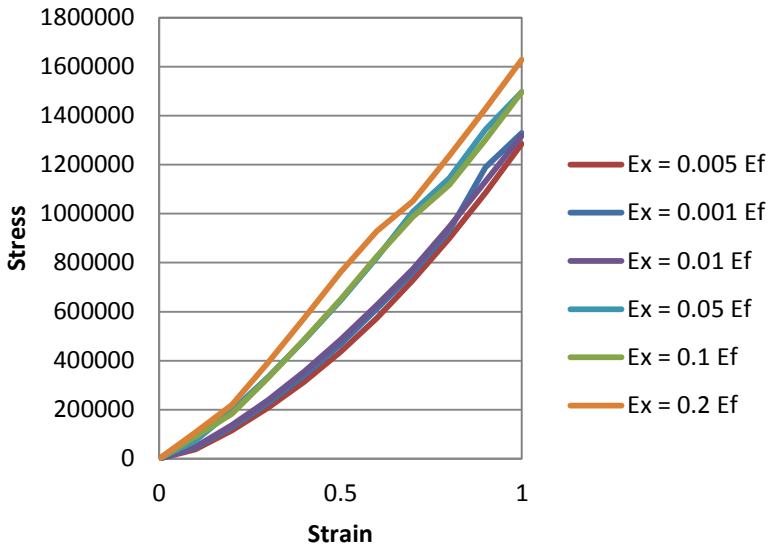

Figure 20: Stress Strain Relationships Corresponding to Relative Cross Link Stiffness

The above plot shows the general J shaped stress strain curve that has been shown to explain the behavior of collagen gels under tension in various experiments, most notably in Xu et al. 2011. The J shaped curve explains the material response of individual collagen fibers realigning to the direction of their applied force. This can be visualized by changing θ in Equation 32. For example, if the RVE is being stretched in the y direction, the fibers will realign themselves closer to this direction. This means that θ will approach 90 degrees, thereby shrinking the cosine terms and growing the sin terms. As the sin terms increase, the stiffness of the element in the y direction also increases [6], [13], [16], [2].

The fracture point of a collagenous tissue occurs when a mechanism is formed through the failure of fibers and cross links. It is pointed out in Buehler 2008 that the response to failure of collagen systems is quite brittle once a failure criterion has been reached. The proposed RVE follows this behavior, as can be seen in the below figure. In this figure, intact fibers are represented by black lines. Intact cross links are represented by blue lines. Fibers and cross links that have reached their failure criteria are represented by red lines. The second plot shows the J shaped stress strain curve that flattens out before brittle failure of the material [13].

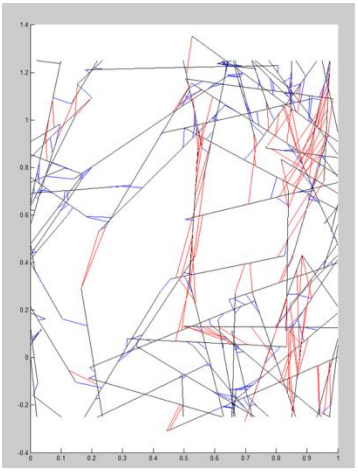

a

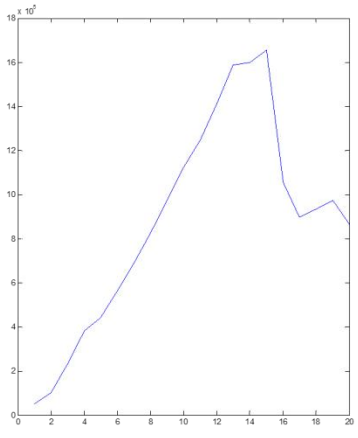

b

Figure 21: a) RVE Showing Broken Fibers and Cross Links. b) Stress-Strain Plot and Failure Region of Failed RVE

Conclusions and Further Research

It is shown by the results of the coded RVE that the behavior of collagen based materials is successfully modeled by truss structures. One of the most important results is the mimicking of the RVE in the J shaped stress strain response of collagen materials. This proves that the model has sufficient fiber realignment when being deformed. The capture of fiber realignment is an important process in the utilization of the model for real life tissues. The model is general enough in that it can be used to model all types of collagenous tissues for both random and oriented networks and still capture accurate behavior. Furthermore, the use of truss elements allows for computational efficiency when running models with exceptionally high fiber density. This allows the model to be run on a processor with much less power than would be required for beam elements. The computational efficiency of the model also makes it a good candidate for use in multiscale adaptive refinement models. These adaptive refinement models potentially utilize dozens of microscopic RVE's. Reducing the computational time for one RVE can significantly reduce the computational time for a multiscale model.

It is recommended that further research be done with both the proposed truss model as well as revisions to the model. The model could be revised to be more complete by changing the behavior of the fibers from truss elements to beam elements. This behavior would technically be more accurate, but computationally and conceptually more expensive. Another revision to the model would be to develop domains beyond just rectangles. Cells and tissues have many different shapes and configurations. To completely mimic the behavior of biological materials, their domain must be more accurately represented. Crack propagation through the micro model could potentially be modeled with this RVE. Testing the model with crack propagation would require a large number of fibers in the network. If successfully implemented, a sensitivity analysis on parameters such as fiber anisotropy, average fiber length and cross link stiffness could be run. This sensitivity analysis would look to see which combination of parameters produces the least amount of crack propagation through the material, thereby increasing the fracture toughness of the material. The fracture toughness, or "J" integral is one of the most important parameters in the engineering of new materials. If certain parameters can be optimized for the "J" integral through numerical modeling, gels can be tested with said parameters, and eventually new tissues can be developed for biomedical purposes.

Works Cited

[1] P. F. (ed.), Collagen: Structure and Mechanics, Springer Science+Business Media, 2008.

[2] M.-J. c. a. Y. Z. Bin Xu, "Experimental and Modeling Study of Collagen Scaffolds with the Effects of Crosslinking and Fiber Alginement," *International Journal of Biomaterials,* vol. 2011, pp. 1-12, 2011.

[3] G. Holzapfel, "Biomechanics of Soft Tissue," *Computational Biomechanics,* vol. 14B, p. 15, 2000.

[4] S. M. Klisch and J. C. Lotz, "Application of a fiber-reinforced continuum theory to multiple deformations of the annulus fibrosus," pp. 1-10, 1999.

[5] B. Agoram and V. H. Barocas, "Coupled Macroscopic and Microscopic Scale Modeling of Fibrillar Tissues and Tissue Equivalents," *Journal of Biomechanical Engineering,* vol. 123, pp. 362-369, 2000.

[6] N. K. Simha, M. Fedewa, P. H. Leo, J. L. Lewis and T. Oegema, "A composites theory predicts the dependence of stiffness of cartilage culture tissues on collagen volume fraction," *Journal of Biomechanics,* vol. 32, pp. 503-509, 1999.

[7] Y. Lanir, "Constitutive Equations for Fibrous Connective Tissues," *Journal of Biomechanics,* vol. 16, pp. 5-12, 1982.

[8] D. J. Hulmes, "Building Collagen Molecules, Fibrils and Suprafibrillar Structures," *Journal of Structural Biology,* vol. 137, pp. 2-10, 2002.

[9] W. H. a. R. W. Glanville, "Covalent Crosslinking between Molecules of Type I and Type III Collagen," *European Journal of Biochemistry,* vol. 122, no. 1, pp. 205-213, 1982.

[10] J. C. M. S. a. S. B. Ning pan, "Micromechanics of a Planar Hybrid Fibrous Network," *Textile Research Journal,* vol. 67, no. 12, pp. 907-925, 1997.

[11] R. Y. P. Franck Vernerey, "Analysis of Soft Fibers with Kenematic constraints and Cross-Links by Finite Deformation Beam Theory," *Journal of Engineering Mechanics,* vol. 137, pp. 128-138, 2001.

[12] N. D. L. T. J. S. a. A. J. B. Kay Barnard, "Chemistry of the collagen cross-links," *Biochemistry,* vol. 244, pp. 303-309, 1987.

[13] M. J. Buehler, "Nanomechanics of collagen fibrils under varying cross-link densities: Atomistic and continuum studies," *Journal of the Mechanical Behavior of Biomedical Materials,* pp. 59-67, 2008.

[14] A. M. Sastry, C. W. Wang and L. Berhan, "Deformation and Failure in Stochastic Fibrous Networks: Scale, dimension and Application," University of michigan, Ann Arbor, 2000.

[15] P. S. M. L. R. J. L. W. J.S. Stephens-Altus, "Development of bioactive photocrosslinkable fibrous hydrogels," *Journal of Biomedical Materials Research,* vol. 98A, no. 2, pp. 167-176, 2011.

[16] K. K. Blayne A. Roeder, "Tensile Mechinal Properties of Three-Dimensional Type I Collagen Extracellular Matrices with Varied Microstructure," *Journal of Biomedical Engineering,* vol. 124, pp. 214-222, 2002.

[17] P. L. Chandran and V. H. Barocas, "Deterministic Material-Based Averaging Theory Model of Collagen Gel Micromechanics," *Journal of Biomechanical Engineering,* vol. 129, pp.

137-147, 2007.

[18] B. a. B. I. Szabo, Finite Element Analysis, John Wiley & Sons, 1991.

[19] D. Roylance, "Finite Element Analysis," Cambridge, MA, 2001.

[20] J. M. W. J. Cantwell, "The impact resistance of composite materials-a review," *Composites,* vol. 22, no. 5, pp. 347-362, September 1991.

[21] C. W. Wang, L. Berhan, Sastry and M. A., "Structure, Mechanics and Failure of Stochastic Fibrous Networks: Part I--Microscale Considerations," *Journal of Engineering Materials and Technology*, pp. 450-459, 2000.

[22] T. Stylianopoulos and V. H. Barocas, "Volume-averaging theory for the study of the mechanics of collagen networks," *Computer methods in applied mechanics and engineering*, vol. 196, pp. 2981-2990, 2007.

[23] D. Roylance, "Overview of Fiber-Reinforced Composites," 2011. [Online]. Available: http://web.mit.edu/course/3/3.064/OldFiles/www/. [Accessed 8 September 2011].

[24] C. W. Wang and A. M. Sastry, "Structure, Mechanics and Failure of Stochastic Fibrous Networks: Part II--networkd Simulations and Application," *Journal of Engineering Materials and Technology*, vol. 122, pp. 460-468, 2000.

[25] S. V. A. R. M. J. B. Alfonso gautieri, "Hierarchal Structure and Nanomechanics of Collagen Microfribrils from the Atpmistic Scale Up," *Nano Letters*, vol. 11, pp. 757-766, 2011.

[26] R. B. M. J. B. a. S. J. E. Yuye Tang, "Deformation micromechanisms of collagen fibrils under uniaxial tension," *Journal of the Royal Society Interface*, vol. 390, pp. 839-850, 2010.